Brief Communication

Effect of Confinement in High-Speed Reacting Mixing Layer

DEBASIS CHAKRABORTY,*† H. S. MUKUNDA, and P. J. PAUL
Department of Aerospace Engineering, Indian Institute of Science, Bangalore 560 012, India

INTRODUCTION

High Mach number mixing layers play an important role in the development of supersonic combustor ramjet (scramjet) engines. The mixing of air and fuel is hindered by both shorter combustor residence time and by stability of supersonic shear layer relative to subsonic counterpart. Although many experimental and computational investigations were carried out for supersonic free shear layer [1–5] and confined shear layer [6–9], the effect of lateral confinement on supersonic mixing layer is not clearly brought out. The fundamental difference in the development of turbulence in the mixing layer and wall boundary layer can affect the structure of the flow and the growth rate of mixing layer significantly. Chakraborty et al. [9] have performed two-dimensional direct numerical simulation (DNS) for high-speed confined reacting shear layer with finite rate chemical kinetics with seven species and seven reactions. Arguments have been provided for treating two-dimensional calculation using the work of Lu and Wu [8], Zhuang et al. [10], Farouk et al. [7], and others who have conducted computational study of the compressibility of high-speed mixing layer and shown that two-dimensional simulation is satisfactory for confined mixing layer. Good comparison of experimental wall pressure distribution with DNS results obtained was considered the basis of further investigations.

In this work, the effect of lateral wall confinement on the growth and structure of supersonic reacting mixing layer has been studied by conducting DNS study for free shear layer and comparing these results with the DNS results of confined shear layer.

*Corresponding author. E-mail: mukunda@cgpl.iisc.ernet.in
†Scientist/Engineer, Aerodynamics Division, VSSC, Thiruvananthapuram.

0010-2180/00/$–see front matter
PII S0010-2180(99)00154-6

ANALYSIS

In order to understand the combustion process inside the scramjet combustor, DNS is performed for the confined supersonic reacting mixing layer as it contains all the fundamental processes involved in supersonic combustion in a confined environment. The results of the DNS calculations for the H_2/air confined supersonic mixing layer are given in the earlier work of the present authors [9]. The simulation is performed for the hypervelocity mixing layer experiment of Erdos et al. [6]. In this experiment, the secondary stream (H_2) comes in contact with the primary stream (air) at the edge of the splitter plate in an enclosed test section of size 535 mm $\times$ 25.4 mm. The schematic experimental setup for which the computations were carried out is presented in Fig. 1. The Mach number and the temperature of the two streams are 3.99 and 2400 K (air) and 3.09 and 103 K (H_2) respectively. The convective velocity is 3000 m/s and the convective Mach numbers are 0.85 and 0.82 referred to H_2 and air streams respectively. The free shear layer experiments of Clemens and Mungal [11] suggest dominant three-dimensional effects for this convective Mach number range and have been supported by linear instability analyses [12, 13] which have shown that oblique disturbances become more and more unstable as convective Mach number exceeds 0.6. However, Tam and Hu [14] and Zhuang et al. [10] have shown that, for laterally confined mixing layers, the most unstable mode is the lowest order two-dimensional mode. The principal point made in these papers is that the coupling between the motion of the shear layer and the channel acoustic wave produces a new instability mechanism in the supersonic range which originates from the wall confinement and is different from the classical Kelvin-Helmholtz

COMBUSTION AND FLAME 121:386–389 (2000)

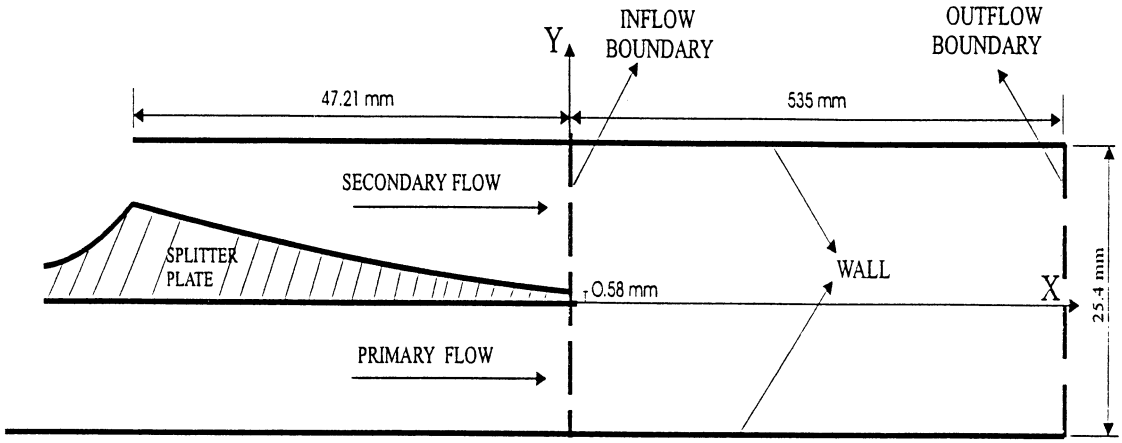

Fig. 1. Schematic representation of experimental setup of Erdos et al. [6] for which computations were done.

instability. Zhuang et al. [10] have shown that the bounded two-dimensional modes are in good agreement with the experiments of Papamoschou and Roshko [15]. Lu and Wu [8] have performed two-dimensional simulations for a mixing layer with a convective Mach number as high as 1.77 citing the work of Tam and Hu [14] who studied the effect of confinement on the shear layer development in supersonic streams. These studies have shown that two-dimensional simulation is satisfactory for confined mixing layers.

Two-dimensional simulations by Liou et al. [5] have been shown to capture the major features of supersonic free shear layer for the higher convective Mach numbers also. Further, Shin and Fergizer [16] demonstrated that heat release makes the dominant mode two-dimensional even in the high Mach number region and concluded that the most unstable mode for reacting flow is two-dimensional even if the instability mode is three-dimensional (oblique) for the nonreacting case. So the role of large-scale structure in the development of supersonic reacting mixing layer is very important and can be understood from two-dimensional simulation. Effect of lateral confinement on the growth of the supersonic reacting mixing layer is investigated by comparing the two-dimensional DNS results of free and confined cases.

TABLE 1

Inflow Parameters for Reacting Mixing Layer

Species	u, km/s	T, K	M	p, MPa	Re/mm
H_2	2.4	103	3.09	0.021	1,600
Air	3.8	2,344	3.99	0.021	22,000

The details of the computational procedure are available in Ref. [9]. Two-dimensional Navier-Stokes equations along with species continuity equations are discretized by a fourth-order spatial and second-order temporal compact scheme [17, 18]. The chemistry model includes six reacting species H_2, O_2, H_2O, OH, H, O and nonreacting species N_2 and seven reaction mechanisms [17]. The species HO_2 and H_2O_2, important in ignition are not included in the mechanism. This is because the present study is aimed at examining the effect of lateral confinement on the growth rate of supersonic mixing layer. The grid structure has 1000 grid points of 0.3 to 0.8 mm size along the length of 535 mm, while the smaller size is arranged near the inflow plane to capture initial development of the mixing layer. There are 101 grid points in the cross stream direction with fine grid (of size 0.09 mm) near the interface, and the grid is exponentially stretched in the far field region toward upper and lower boundaries. Grid independence of the results was established by comparing spatial profiles with different grids and also by analyzing the spectral content of fluctuations of the flow parameters.

Application of the boundary conditions for the free shear layer problem differs from the boundary conditions for the confined case [9]. The solid walls (both upper and lower) for the confined case is replaced by free surface bound-

aries. The conditions at free surfaces are obtained by solving Riemann conditions. On the inflow streams is imposed a velocity fluctuation over a range of frequencies at a total rms intensity of 0.3% of the mean velocity (See Table 1 for Pa stream parameters.). This frequency range allows the mixing layer to grow as may happen in reality. The outflow boundary conditions are obtained by second-order extrapolation and are considered satisfactory for this problem dominated by supersonic flow.

RESULTS AND DISCUSSION

As in the earlier study [9], the computations were performed for three sweep times—one sweep for clearing the flow field and two more sweeps to collect statistical information and also to check on the statistical invariance of the calculation. One sweep of calculation is taken as the time the flow takes to cross the axial length of flow domain (535 mm) with its convective velocity. After the attainment of statistical steady state, velocities, density, and the species mass fractions are gathered at all radial points of few axial locations at each time step over one sweep duration to enable statistical analysis.

The mean profiles of axial velocity (u) and density (ρ) at various axial locations are first calculated from the stored time series data of DNS. Two different estimates, namely shear layer thickness (b) and momentum thickness (θ), were made from these mean profiles for calculation of shear layer width. The shear layer thickness (b) is defined as the distance of the transverse locations where the value of $|(u - u_a)/(u_a - u_b)|$ is 0.9 and 0.1, where u_a and u_b are the velocities of upper and lower streams.

Perhaps a better physical representation of the local width of the mixing layer is provided by the momentum thickness (θ) defined by

$$\theta = \int_{-\infty}^{\infty} \frac{\rho}{\rho_a} u^*(1 - u^*)\, dy \qquad (1)$$

where $u^* = (u - u_b)/(u_a - u_b)$.

Calculated shear layer thickness and momentum thickness for confined and free shear layers are compared in Fig. 2. It is clear that the growth rate is more for confined shear layer

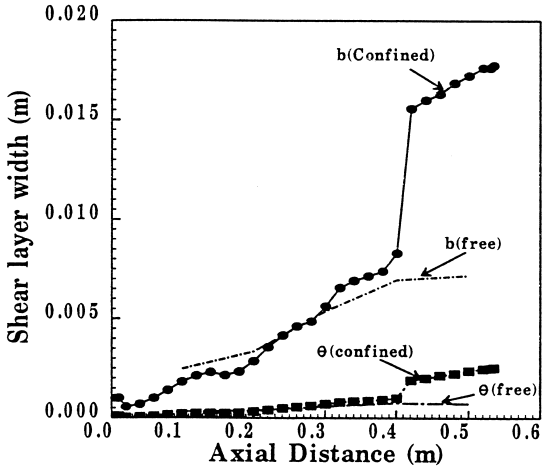

Fig. 2. Comparison of the shear layer growth between the confined and free reacting mixing layer of H_2–air.

compared to free shear layer. Adverse pressure gradient present in wall boundary layer is mainly responsible for the enhanced growth rate of the confined shear layer. Moreover, it is also clear from the figure that up to a distance of 300 mm from the splitter plate, the growth rates for both cases follow the same trend and only beyond that distance the two differ. For the confined mixing layer case, as the flow proceeds downstream, the mixing layer starts coming closer to the boundary layer and there is mutual interference. Further downstream these two layers merge into one another and it is difficult to distinguish between the two. At the farthest downstream location, the width of shear layer for the confined case is about 130% more than that of free shear layer.

The mean mass fractions of H_2O and OH species were compared for both cases in Fig. 3 at the axial locations of 100 mm, 300 mm, and 500 mm. It is clear from the figure that up to a distance of 300 mm the reaction zone for both the free and confined shear layers is limited to the mixing layer region. Further downstream, for the confined case, because of merging of the mixing layer and wall boundary layers the reaction zone for the confined case extended up to the lower wall and it is about 5% more than the free shear layer reaction zone. Higher temperature in the wall boundary layer of the confined flow aids reaction and causes this broader reaction zone.

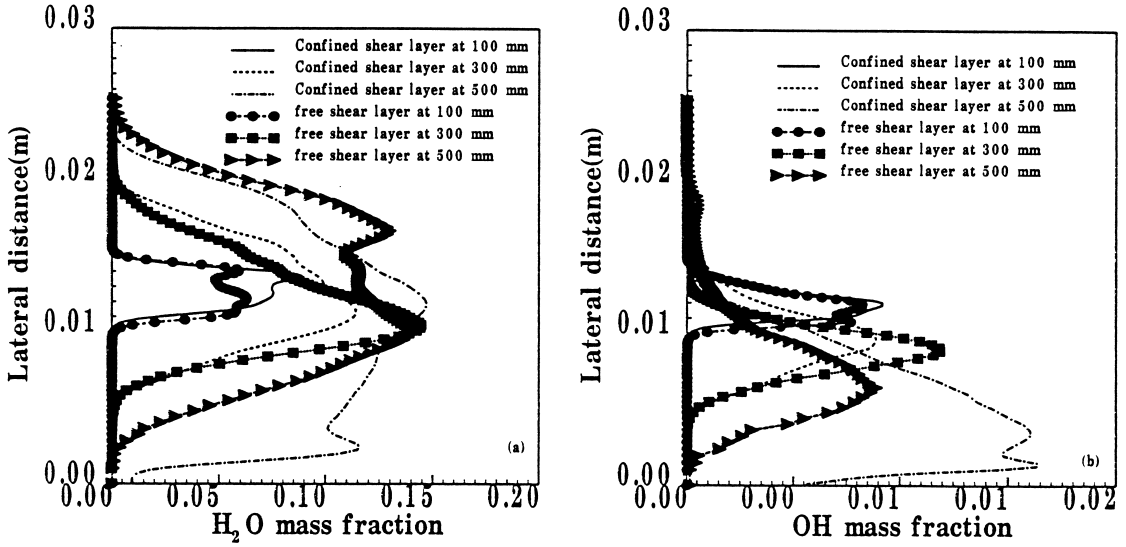

Fig. 3. Comparison of mean profiles at various axial locations for confined and free mixing layers (a) H_2O mass fraction, (b) OH mass fraction.

CONCLUSIONS

The effect of lateral confinement on the growth and structure of hypersonic reacting mixing layer has been studied by comparing DNS results of confined and free shear layers for the same inflow parameters. It is observed that because of the presence of adverse pressure gradient in the wall boundary layer, the growth rate of the confined mixing layer is much greater compared to the free shear layer, although the growth rates of the two follow the same trend until there exists distinct mixing layer and wall boundary layer. The presence of higher temperature in wall boundary layer causes a broader reaction zone for the confined case compared to free shear layer.

The authors would like to express their sincere thanks to Dr. V. Adimurthy of VSSC, Thiruvananthapuram for the support provided for carrying out this work.

REFERENCES

1. Clemens, N. T., and Mungal, M. G., *AIAA J*. 30:973–981 (1992).
2. Elliott, G. S., Saminy, M., and Arnett, S. A., *Phys. Fluids* 7:864–876 (1995).
3. Sekar, B., and Mukunda, H. S., *Twenty-Third Symposium (International) on Combustion*, The Combustion Institute, Pittsburgh, 1990 pp. 707–713.
4. Mukunda, H. S., *Combust. Sci. Technol*. 89:285–290 (1992).
5. Liou, T., Lien, W., and Huang, P. *AIAA J*. 33:2332–2338 (1995).
6. Erdos, J., Tamagno, J., Bakos, R., and Trucco, R. (1992). AIAA-92-0628.
7. Farouk, B., Oran, E. S., and Kailashnath, K., *Phys. Fluids A* 3:2786–2798 (1991).
8. Lu, P. J., and Wu, K. C., *Phys. Fluids A* 3:3063–3069 (1991).
9. Chakraborty, D., Nagraja Upadhyaya, H. V., Paul, P. J., and Mukunda, H. S., *Phys. Fluids* 9:3513–3522 (1997).
10. Zhuang, M., Dimotakis, P. E., and Kubota, T., *Phys. Fluids A* 2:599–604 (1990).
11. Clemens, N. T., and Mungal, M. G. (1990). AIAA-90-1978.
12. Ragab, S. A., and Wu, J. L., *Phys. Fluids A* 1:957–966 (1989).
13. Sandham, N. D., and Reynolds, W. C., *AIAA J*. 28: 618–622 (1990).
14. Tam, C. K. W., and Hu, F. Q., *J. Fluid Mech*. 203:51–76 (1989).
15. Papamoschou, D., and Roshko, A., *J. Fluid Mech*. 197:453–457 (1988).
16. Shin, D. S., and Ferziger, J. H., *AIAA J*. 31:677–685 (1993).
17. Drummond, J. P., Carpenter, M. H., and Riggins, D. W., in *High Speed Flight Propulsion System* (S. N. B. Murthy and E. T. Curran, Eds.), *AIAA Progress in Aeronautics and Astronautics*, Washington, D.C., Vol. 137, 1991.
18. Carpenter, M. H., *A Generalized Chemistry Version of SPARK*. NASA-CR-4196, 1988.

Received 22 February 1999; revised 3 August 1999; accepted 18 October 1999